Report

Current Biology

Neural Correlates of Body Integrity Dysphoria

Graphical Abstract

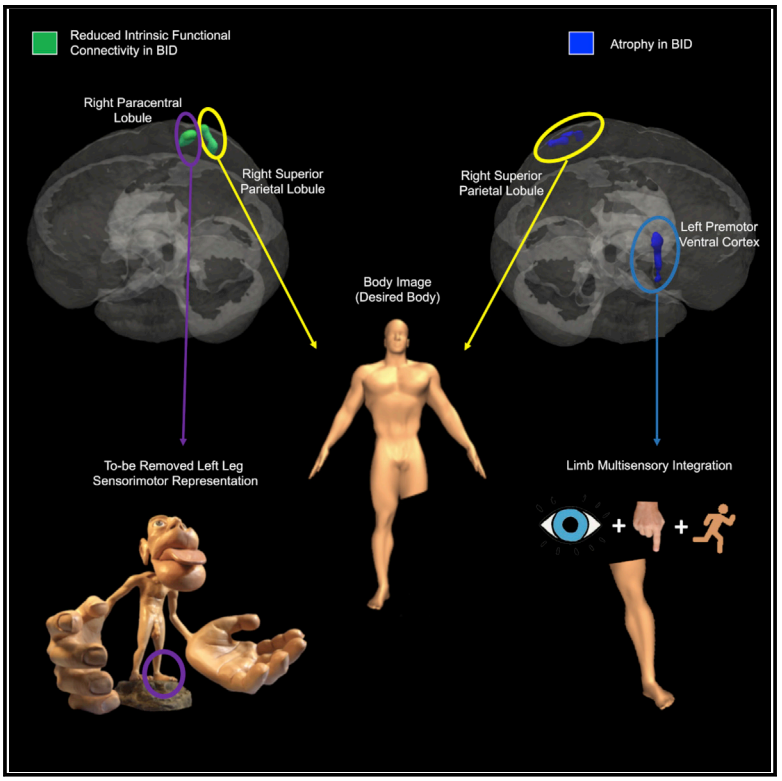

Highlights

- Target limb sensorimotor area shows a breakdown of the functional connectivity
- Left premotor cortex typically involved in limb multimodal integration is atrophic
- Right parietal area representing body shape is structurally and functionally altered
- Atrophy in this right parietal area correlates with simulation of being an amputee

Authors

Gianluca Saetta, Jürgen Hänggi, Martina Gandola, ..., Eraldo Paulesu, Gabriella Bottini, Peter Brugger

Correspondence

gianluca.saetta@gmail.com (G.S.), peter.brugger@kliniken-valens.ch (P.B.)

In Brief

Saetta et al. show that limb ownership depends on (1) the functional connectivity of the brain area containing its primary sensorimotor representation and (2) the structural and functional integrity of areas representing the body as a whole. A breakdown at both levels is observed in persons who aim for the amputation of a healthy limb.

Saetta et al., 2020, Current Biology *30*, 2191–2195
June 8, 2020
https://doi.org/10.1016/j.cub.2020.04.001

CellPress

Current Biology

CellPress

Report

Neural Correlates of Body Integrity Dysphoria

Gianluca Saetta,[1,2,*] Jürgen Hänggi,[1] Martina Gandola,[3,4] Laura Zapparoli,[5,6] Gerardo Salvato,[3,4,10] Manuela Berlingeri,[4,7,8] Maurizio Sberna,[9] Eraldo Paulesu,[5,6] Gabriella Bottini,[3,4,10] and Peter Brugger[2,11,12,*]

[1]Department of Psychology, University of Zurich, Binzmühlestrasse 14, 8050 Zürich, Switzerland
[2]Department of Psychiatry, Psychotherapy and Psychosomatics, Zurich Psychiatric University Hospital, Lenggstrasse 31, 8008 Zürich, Switzerland
[3]Department of Brain and Behavioral Sciences, University of Pavia, Piazza Botta, 27100 Pavia, Italy
[4]NeuroMi, Milan Center for Neuroscience, Piazza dell'Ateneo Nuovo 1, 20126 Milan, Italy
[5]Department of Psychology, University of Milano-Bicocca, Piazza dell'Ateneo Nuovo 1, 20126 Milan, Italy
[6]fMRI Unit, IRCCS Istituto Ortopedico Galeazzi, Via Riccardo Galeazzi 4, 20161 Milan, Italy
[7]Department of Humanistic Studies, University of Urbino Carlo, Via Bramante 17, 61029 Urbino, Italy
[8]Center of Developmental Neuropsychology, ASUR Marche, Area Vasta 1, 61122 Pesaro, Italy
[9]Neuroradiology Department, ASST Grande Ospedale Metropolitano Niguarda, Piazza dell'Ospedale Maggiore 3, 20162 Milan, Italy
[10]Cognitive Neuropsychology Centre, ASST Grande Ospedale Metropolitano Niguarda, Piazza dell'Ospedale Maggiore 3, 20162 Milan, Italy
[11]Neuropsychology Unit, Valens Rehabilitation Centre, Taminaplatz 1, 7317 Valens, Switzerland
[12]Lead Contact
*Correspondence: gianluca.saetta@gmail.com (G.S.), peter.brugger@kliniken-valens.ch (P.B.)
https://doi.org/10.1016/j.cub.2020.04.001

SUMMARY

There are few things as irrefutable as the evidence that our limbs belong to us. However, persons with body integrity dysphoria (BID) [1] deny the ownership of one of their fully functional limbs and seek its amputation [2]. We tapped into the brain mechanisms of BID, examining sixteen men desiring the removal of the left healthy leg. The primary sensorimotor area of the to-be-removed leg and the core area of the conscious representation of body size and shape (the right superior parietal lobule [rSPL]) [3, 4] were less functionally connected to the rest of the brain. Furthermore, the left premotor cortex, reportedly involved in the multisensory integration of limb information [5–7], and the rSPL were atrophic. The more atrophic the rSPL, the stronger the desire for amputation, and the more an individual pretended to be an amputee by using wheelchairs or crutches to solve the mismatch between the desired and actual body. Our findings illustrate the pivotal role of the connectivity of the primary sensorimotor limb area in the mediation of the feeling of body ownership. They also delineate the morphometric and functional alterations in areas of higher-order body representation possibly responsible for the dissatisfaction with a standard body configuration. The neural correlates of BID may foster the understanding of other neuropsychiatric disorders involving the bodily self. Ultimately, they may help us understand what most of us take for granted, i.e., the experience of body and self as a seamless unity.

RESULTS AND DISCUSSION

Human beings commonly experience their bodily self as lying within clearly circumscribed borders defined by biological and societal norms. Paradoxically, in persons with body integrity dysphoria (BID), the desired amputation would make those concerned with the condition "feel more complete" and those having reached an amputated state only regret not having realized it earlier [8]. Two behavioral features are almost invariably associated with the condition, albeit to varying degrees: (1) an erotic attraction to (lower limb) amputees and (2) the habitual simulation of the desired body state by using crutches or wheelchairs ("pretending behavior") [9]. Despite the rarity of this condition, we succeeded in recruiting sixteen men who all desired an amputation of specifically and exclusively the left leg. None had any history of major psychiatric or neurologic disorders. BID participants were compared to sixteen healthy control men matched for age and formal education. Pinpointing the differences in the functional and structural architecture between BID individuals and control persons' brains provided the unique opportunity to reveal the neural networks involved in the sense of ownership of a limb as an integral part of the body. Moreover, it allowed us to identify the candidate brain areas underlying the satisfaction of possessing a determined body configuration. In particular, in BID individuals, we explored (1) alterations in intrinsic functional connectivity in cortical hubs (i.e., small multimodal areas reached by many functional connections disproportionate to their spatial extension) [10–12] and (2) structural atrophies or hypertrophies in the functionally altered regions as well as in other specific candidate regions [5, 13]. Alterations in functional connectivity and the concentration of gray matter were related to the self-reported characteristics of an individual's amputation desire, as carefully assessed in a clinical interview.

Cortical hubs with reduced intrinsic functional connectivity in BID compared with controls were the right paracentral lobule (rPCL), the right superior parietal lobule (rSPL), the pars orbitalis

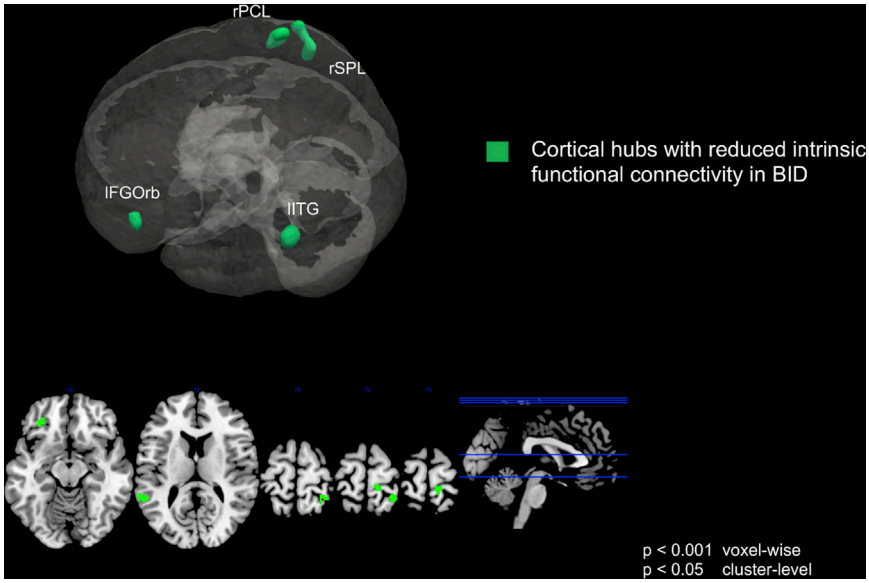

Figure 1. Reduced Intrinsic Connectivity of Cortical Hubs in BID

Results are extracted at $p < 0.001$ voxel-wise and $p < 0.05$ cluster level (not corrected). lIFGOrb, pars orbitalis of the left inferior frontal gyrus; rPCL, right paracentral lobule; rSPL, right superior parietal lobule; lITG, left inferior temporal gyrus.

of the left inferior frontal gyrus (lIFGOrb), and the left inferior temporal gyrus (lITG). Results are shown in Figure 1 and Table 1. The areas with a reduced concentration of gray matter in BID compared with controls were the rSPL, the left premotor cortex (lPMv), and the lIFGOrb. Results are shown in Figure 2 and Table 1. The concentration of gray matter in the rSPL negatively correlated with the strength of the desire for amputation (Pearson's correlation coefficient; $r_{(14)} = 0.51$; $p = 0.01$) and the pretending behavior (Pearson's correlation coefficient; $r_{(14)} = 0.62$; $p = 0.01$; see also Figure 2), as assessed by the respective subscores at the Zurich Xenomelia Scale [14].

The rPCL, which houses the primary somatosensory representation of the affected left leg, showed a reduced intrinsic functional connectivity to other cortical regions. Remarkably, no *structural* alterations were evident in the rPCL, which is in line with a normal neurological status examination, specifically showing unimpaired tactile and motor functioning of BID individuals' left leg. The rSPL showed both reduced intrinsic functional connectivity and concentration of gray matter. The absence of any neurological deficits or BID-related symptoms for the right leg and both the upper limbs suggests a specificity of these alterations for the desired removal of the left leg. Our results support the view that the distressing feeling of non-acceptance of one's limb in BID might ensue from a discrepancy between preserved projections of somatosensory inputs from the limb to the respective primary cortical areas and an impaired representation of the body at the highest level of integration, the so-called body image [3]. That is the representation of the size, shape, and physical composition of the body, i.e., "the conscious body image" [15–17]. The rSPL was previously identified as a critical hub for the body image [3, 4]. Specifically, a magnetoencephalography study showed that, in BID individuals, the tactile stimulation of the to-be-removed limb was accompanied by reduced activation of the rSPL [3]. Likewise, a surface-based morphometry investigation reported a reduced thickness of rSPL in association with BID [13]. Body image arises from the integration of multiple sensory inputs (i.e., visual, tactile, proprioceptive, vestibular, and re-afferent motor signals). It is thought to be scaffolded by the activity of distributed neural networks whose integrity is responsible, on a phenomenal level, for an individual's perception of his or her own body as coherent and unitary [17]. A central region for multisensory integration, the lPMv [6], was found atrophic in the BID individuals examined here. The lPMv binds together visuomotor and tactile information about a limb through its anatomical connections to frontoparietal areas [18]. A specific role of the lPMv in multisensory integration and limb ownership was already suggested in previous studies on BID [5, 7]. Blood-oxygen-level-dependent (BOLD) activity in the lPMv was decreased in 5 individuals with BID during the touch of the desired-to-be-removed compared to the accepted limb [7]. Atrophies in the lPMv have been described in a subsequent study [5].

Previous studies, cited above, were preliminary in that a small number of BID individuals with an amputation desire targeting different limbs had been recruited. Moreover, these studies investigated either functional characteristics [3, 7], connectivity [19], or morphometry [5, 13] of BID individuals' brains separately. The novelty of the present approach consists in the combination of morphometric (gray matter density) and functional connectivity analyses within one relatively large and homogeneous sample. The results produced by previous studies also did not survive

Table 1. Reduced Intrinsic Connectivity of the Cortical Hubs, Atrophies, and Hypertrophy in BID

	MNI Coordinates							
	Left Hemisphere				Right Hemisphere			
Brain Regions (BA)	x	y	z	*Z* Score	x	y	z	*Z* Score
Reduced Intrinsic Connectivity of the Cortical Hubs in BID								
Inferior orbitofrontal gyrus	−32	36	−12	4.23				
Paracentral lobule					10	−38	78	4.04
Superior parietal lobule					22	−52	60	3.79
Inferior temporal gyrus	−60	−44	16	4.16				
Atrophies in BID								
Inferior orbitofrontal gyrus	−36	36	−9	6.05				
Precentral gyrus	−38	2	34	5.63				
Precentral gyrus	−50	2	27	4.82				
Superior parietal lobule					39	−56	57	6.5
Hypertrophy in BID								
Middle temporal gyrus	−60	4	−21	6.3				

MNI, Montreal Neurological Institute

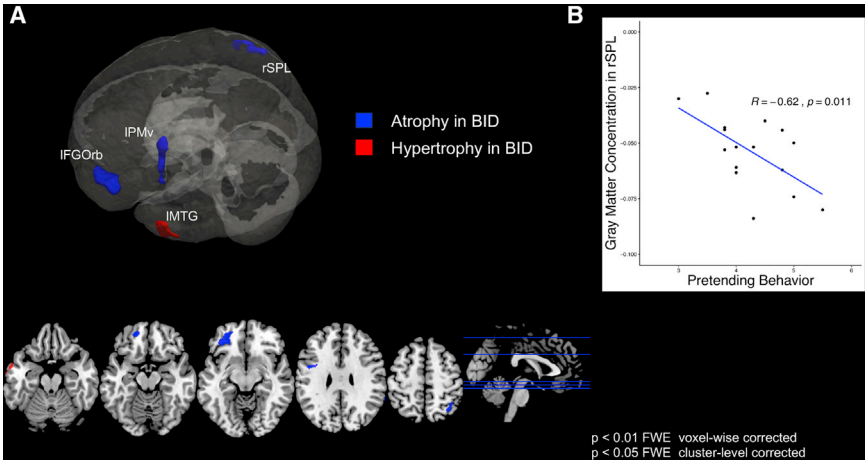

Figure 2. Atrophies and Hypertrophy in BID

(A) Atrophic and hypertrophic areas in BID. Results are extracted at p < 0.01 FWE voxel-wise corrected and k > 25.

(B) Scatterplot of the correlation between the concentration of gray matter in the rSPL at [X = 39, Y = −56, Z = 57] and the pretending behavior in BID individuals. On the y axis, the contrast values (reduced concentration of gray matter in BID individuals compared to controls) are reported. IPMv, left ventral premotor cortex; IMTG, left middle temporal gyrus; IFGOrb, inferior frontal gyrus; pars orbitalis; rSPL, right superior parietal lobule.

conservative statistical thresholding. Here, results were extracted at $p < 0.001$ uncorrected at the voxel-wise level and $p < 0.05$ at the cluster level to identify the cortical hubs presenting altered functional connectivity in BID (listed in Table 1 and displayed in Figure 1). Regional gray matter reductions in BID were explored by applying the most conservative thresholding method available in SPM ($p < 0.05$ FWE voxel-wise corrected) coupled with a cluster-extent threshold of $k > 25$ to further exclude spurious findings. The results are listed in Table 1 and displayed in Figure 2. Our findings, combined with the integration of results from previous studies, allow the formulation of an evidence-based, comprehensive model of the neural networks implicated in BID. According to this model, BID might be characterized at a neural level by (1) insufficient anchoring of limb representations as suggested by the lack of intrinsic functional connectivity in the rPCL; (2) a deficit in multimodal integration, as indicated by structural anomalies of the lPMv and rSPL; and (3) altered body image in the rSPL, reflected by both functional and structural abnormalities of this region.

Body image in the rSPL has been proposed to be genetically determined [20]. A proof of concept might be the observation of phantom limb sensations in amelia, i.e., the phenomenal existence of a limb despite its physical absence in humans born without the respective limb [21]. It was previously shown that an amelic individual imagining or executing phantom limb movements activated no primary sensory and motor areas but the rSPL [21]. BID and amelia might share a common altered developmental mechanism responsible for the discrepancy between physical and phenomenal body states [22]. This perspective becomes more compelling when taking into account our finding of an association between rSPL architecture and the strength of the amputation desire on the one hand and inclination to pretending behavior on the other hand. Specifically, the more atrophic rSPL, the stronger the desire for amputation, and the more a BID individual would mimic the status of an amputee. Alteration of the rSPL might be the neural substrate of a BID individual's unusual body image. The pretending behavior could represent the attempt to solve the mismatch between the experienced and the desired body. The transient alleviation of the desire for amputation obtained by binding up the leg or sitting in a wheelchair might stem from the alignment of the actual visual information about a temporary amputated body state and the individual's body image that lacks a limb. Accordingly, Stone et al. [23] induced in BID individuals the illusory experience of the affected limb to fade off from visual awareness. This gave them instant relief from their symptoms, if only transiently. Other evidence that body image is built up at a very early stage of development is that the experience of BID typically lasts as long as an individual can remember. The characteristics of the desire for amputation (i.e., the affected limb, the exact demarcation line, etc.) usually remain stable across a BID individual's lifespan. Pretending behavior might thus correspond to acting out a possibly innate, individually shaped body image.

Oddo et al. [24] recently presented BID individuals and controls with morphs depicting either the observer's actual or amputated body. In that study, multivariate statistics using machine learning were able to discriminate between a BID group and a control group based on the BOLD signal in the rSPL. In line with previous reports [25], BID individuals rated pictures of amputated bodies as more pleasant and sexually arousing than those of intact bodies. Taken as a whole, these findings might suggest an interdependence between a person's bodily self and her sexual orientation along the spectrum of bodily appearance. From a neural point of view, Ramachandran et al. [4] proposed the possible existence of a genetically determined cortical template of body image hard-wired into the rSPL. Such a template would shape the connections within the limbic system, promoting an individual to be attracted erotically toward body shapes that match those contained in this template. Therefore, donkeys prefer other donkeys as sexual partners, and humans prefer other humans. BID individuals, whose body image lacks a limb, prefer amputees. Indeed, the majority of BID individuals with a desire for lower limb amputations are also attracted to *lower* limb amputees [4]. In line with Ramachandran's intuition, we found that, in persons with BID, the lIFGOrb, which belongs to the limbic system, showed both reduced intrinsic functional connectivity and concentration of gray matter. Future studies should tap into the cerebral networks for body image and erotic attraction to bodily appearance, examining in more detail the possible relationship between the rSPL, the lIFGOrb, and the limbic system.

The empirical approach taken in the present study illustrates that the bodily self critically depends on the functional connectivity of the limb primary sensorimotor area rather than its structural properties. However, at higher levels of bodily representation, both functional connectivity *and* gray matter characteristics of multimodal integration hubs seem to be necessary for a healthy binding of body and self. Only a smooth interplay between low-

Table 2. Characteristics of the Participants with BID

Participant	Age (Years)	Education (Years)	Scanner (Place)	Mean Scores on Zurich Xenomelia Scale (SD)			
				Subscale "Amputation Desire"	Subscale "Erotic Attraction"	Subscale "Pretending Behavior"	Total Scale Score
1	36	13	Milan	4.5 (2.4)	4.3 (2.4)	5.0 (2.0)	4.6 (2.1)
2[a]	36	13	Milan	5.3 (1.5)	3.3 (1.5)	3.0 (0.8)	3.8 (1.6)
3	48	18	Milan	6.0 (0.0)	3.5 (1.7)	4.0 (2.3)	4.5 (1.9)
4	34	18	Milan	5.3 (0.5)	2.8 (1.3)	3.3 (2.1)	3.8 (1.7)
5	37	18	Milan	6.0 (0.0)	6.0 (0.0)	4.8 (1.9)	5.6 (1.2)
6	41	13	Milan	6.0 (0.0)	4.3 (2.4)	5.5 (1.0)	5.3 (1.5)
7	39	18	Milan	5.8 (0.5)	4.5 (1.0)	5.0 (2.0)	5.1 (1.3)
8	64	13	Milan	6.0 (0.0)	5.5 (1.0)	4.5 (2.4)	5.3 (1.5)
9	41	18	Zurich	5.8 (0.5)	4.3 (2.4)	3.8 (2.6)	4.6 (1.7)
10[a]	46	18	Zurich	4.0 (1.8)	5.3 (1.5)	4.3 (1.5)	4.5 (0.2)
11	63	16	Zurich	5.5 (1.0)	2.5 (1.0)	4.0 (2.5)	4.0 (0.8)
12	57	18	Zurich	5.5 (1.0)	3.8 (1.5)	3.8 (2.2)	4.3 (0.6)
13	29	18	Zurich	5.0 (1.4)	6.0 (0.0)	4.3 (2.2)	5.1 (1.1)
14	28	18	Zurich	5.5 (1.0)	6.0 (0.0)	4.8 (2.5)	5.4 (1.3)
15	44	13	Zurich	5.8 (0.5)	3.3 (1.0)	4.0 (2.2)	4.3 (0.9)
16	67	18	Zurich	5.5 (0.6)	5.8 (0.5)	3.8 (2.6)	5.0 (1.2)

[a]Proceeded to amputation ~1 year after study completion

level and high-level bodily processing makes us feel that single limbs belong to our body as much as to our self. And only such integrity between body and self will guarantee satisfaction in both personal and social life. In this respect, an old but almost forgotten wisdom about the bodily self regains appreciation: "body image is a social phenomenon" [26, p. 217, 27].

Our findings suggest that the desire for amputation in BID individuals might be accounted for specific anomalies in brain architecture. Such a view complements previous conceptualizations of BID as a paraphilia or an Internet-induced madness [2]. The upcoming release of ICD-11 proposes to define BID as a "disorder of bodily distress or bodily experience" [1]. We have outlined here the neural correlates of this "new" condition.

The empirical approach taken in this study is correlational. The neuroimaging methods used here do not allow any inferences on causality. However, facing the graphical depictions of a relationship between cortical structure and behavior, the vector of causality is reportedly biased in a brain-to-mind direction [28]. This holds for laypeople and academics alike and underlines the necessity of considering nonlinear interactions of biological, psychological, and social factors underlying BID. An integrative, cross-disciplinary view might have promising implications for the understanding of neuropsychiatric disorders, such as BID, and will ultimately allow refined definitions of diagnostic criteria.

STAR★METHODS

Detailed methods are provided in the online version of this paper and include the following:

- KEY RESOURCES TABLE
- RESOURCE AVAILABILITY
  - Lead Contact
  - Materials Availability
  - Data and Code Availability
  - Subjects Details
- METHOD DETAILS
  - Clinical assessments and questionnaires
  - Magnetic resonance imaging data acquisition in Zurich
  - Magnetic resonance imaging data acquisition in Milan
- QUANTIFICATION AND STATISTICAL ANALYSIS
  - Rs-fMRI Data preprocessing
  - Intrinsic functional connectivity of the cortical hubs
  - The BID Mask
  - Voxel-based Morphometry analysis

ACKNOWLEDGMENTS

We thank the participants for their time and efforts as they traveled abroad to take part in the study. We thank Dr. Jacob M. Paul for his wise advice on the data analysis and Jasmine Ho for proofreading. This work was supported by the Swiss National Science Foundation projects Sinergia no. 160837 "MeganePro" and Doc.Mobility no. 181383.

AUTHOR CONTRIBUTIONS

G. Saetta wrote the manuscript. P.B., G.B., and E.P. conceptualized the project. G. Saetta, J.H., M.G., L.Z., G. Salvato, and M.S. collected the data. P.B., G.B., G. Saetta, and M.G. performed the clinical interview. G. Saetta performed data analyses. J.H. and M.B. supervised and validated data analyses. All authors approved the final version of the manuscript.

DECLARATION OF INTERESTS

The authors declare no competing interests.

Received: February 20, 2020
Revised: March 31, 2020
Accepted: April 1, 2020
Published: May 7, 2020

REFERENCES

1. World Health Organization (2020). ICD-11 - mortality and morbidity statistics. https://icd.who.int/browse11/l-m/en#/http://id.who.int/icd/entity/256572629.
2. Brugger, P., Christen, M., Jellestad, L., and Hänggi, J. (2016). Limb amputation and other disability desires as a medical condition. Lancet Psychiatry *3*, 1176–1186.
3. McGeoch, P.D., Brang, D., Song, T., Lee, R.R., Huang, M., and Ramachandran, V.S. (2011). Xenomelia: a new right parietal lobe syndrome. J. Neurol. Neurosurg. Psychiatry *82*, 1314–1319.
4. Ramachandran, V.S., Brang, D., McGeoch, P.D., and Rosar, W. (2009). Sexual and food preference in apotemnophilia and anorexia: interactions between 'beliefs' and 'needs' regulated by two-way connections between body image and limbic structures. Perception *38*, 775–777.
5. Blom, R.M., van Wingen, G.A., van der Wal, S.J., Luigjes, J., van Dijk, M.T., Scholte, H.S., and Denys, D. (2016). The desire for amputation or paralyzation: Evidence for structural brain anomalies in Body Integrity Identity Disorder (BIID). PLoS ONE *11*, e0165789.
6. Ehrsson, H.H., Holmes, N.P., and Passingham, R.E. (2005). Touching a rubber hand: feeling of body ownership is associated with activity in multisensory brain areas. J. Neurosci. *25*, 10564–10573.
7. van Dijk, M.T., van Wingen, G.A., van Lammeren, A., Blom, R.M., de Kwaasteniet, B.P., Scholte, H.S., and Denys, D. (2013). Neural basis of limb ownership in individuals with body integrity identity disorder. PLoS ONE *8*, e72212.
8. Noll, S., and Kasten, E. (2014). Body integrity identity disorder (BIID): how satisfied are successful wannabes. Psychol Behav Sci *3*, 222–232.
9. First, M.B., and Fisher, C.E. (2012). Body integrity identity disorder: the persistent desire to acquire a physical disability. Psychopathology *45*, 3–14.
10. Sporns, O., Honey, C.J., and Kötter, R. (2007). Identification and classification of hubs in brain networks. PLoS ONE *2*, e1049.
11. Rubinov, M., and Sporns, O. (2010). Complex network measures of brain connectivity: uses and interpretations. Neuroimage *52*, 1059–1069.
12. Buckner, R.L., Sepulcre, J., Talukdar, T., Krienen, F.M., Liu, H., Hedden, T., Andrews-Hanna, J.R., Sperling, R.A., and Johnson, K.A. (2009). Cortical hubs revealed by intrinsic functional connectivity: mapping, assessment of stability, and relation to Alzheimer's disease. J. Neurosci. *29*, 1860–1873.
13. Hilti, L.M., Hänggi, J., Vitacco, D.A., Kraemer, B., Palla, A., Luechinger, R., Jäncke, L., and Brugger, P. (2013). The desire for healthy limb amputation: structural brain correlates and clinical features of xenomelia. Brain *136*, 318–329.
14. Aoyama, A., Krummenacher, P., Palla, A., Hilti, L.M., and Brugger, P. (2012). Impaired spatial-temporal integration of touch in Xenomelia (body integrity identity disorder). Spat. Cogn. Comput. *12*, 96–110.
15. Gadsby, S. (2019). Body representations and cognitive ontology: drawing the boundaries of the body image. Conscious. Cogn. *74*, 102772.
16. Longo, M.R. (2015). Implicit and explicit body representations. Eur. Psychol. *20*, 6–15.
17. Longo, M.R., Azañón, E., and Haggard, P. (2010). More than skin deep: body representation beyond primary somatosensory cortex. Neuropsychologia *48*, 655–668.
18. Rizzolatti, G., Luppino, G., and Matelli, M. (1998). The organization of the cortical motor system: new concepts. Electroencephalogr. Clin. Neurophysiol. *106*, 283–296.
19. Hänggi, J., Vitacco, D.A., Hilti, L.M., Luechinger, R., Kraemer, B., and Brugger, P. (2017). Structural and functional hyperconnectivity within the sensorimotor system in xenomelia. Brain Behav. *7*, e00657.
20. Ramachandran, V.S., and Hirstein, W. (1998). The perception of phantom limbs. The D. O. Hebb lecture. Brain *121*, 1603–1630.
21. Brugger, P., Kollias, S.S., Müri, R.M., Crelier, G., Hepp-Reymond, M.C., and Regard, M. (2000). Beyond re-membering: phantom sensations of congenitally absent limbs. Proc. Natl. Acad. Sci. USA *97*, 6167–6172.
22. Hilti, L.M., and Brugger, P. (2010). Incarnation and animation: physical versus representational deficits of body integrity. Exp. Brain Res. *204*, 315–326.
23. Stone, K.D., Bullock, F., Keizer, A., and Dijkerman, H.C. (2018). The disappearing limb trick and the role of sensory suggestibility in illusion experience. Neuropsychologia *117*, 418–427.
24. Oddo-Sommerfeld, S., Hänggi, J., Coletta, L., Skoruppa, S., Thiel, A., and Stirn, A.V. (2018). Brain activity elicited by viewing pictures of the own virtually amputated body predicts xenomelia. Neuropsychologia *108*, 135–146.
25. Blom, R.M., van der Wal, S.J., Vulink, N.C., and Denys, D. (2017). Role of sexuality in body integrity identity disorder (BIID): a cross-sectional internet-based survey study. J. Sex. Med. *14*, 1028–1035.
26. Schilder, P. (1935). The Image and Appearance of the Human Body: Psyche Monographs, No. 4 (Lond. Kegal Paul Trench Trubn. Co.).
27. Brugger, P., and Lenggenhager, B. (2014). The bodily self and its disorders: neurological, psychological and social aspects. Curr. Opin. Neurol. *27*, 644–652.
28. Brugger, P., Kurthen, I., Rashidi-Ranjbar, N., and Lenggenhager, B. (2018). Grey matter or social matters? Causal attributions in the era of biological psychiatry. Eur. Psychiatry *52*, 45–46.
29. Whitfield-Gabrieli, S., and Nieto-Castanon, A. (2012). Conn: a functional connectivity toolbox for correlated and anticorrelated brain networks. Brain Connect. *2*, 125–141.
30. Ashburner, J., and Friston, K.J. (2005). Unified segmentation. Neuroimage *26*, 839–851.
31. Wittchen, H.U., Zaudig, M., and Fydrich, T. (1997). Structured Clinical Interview for DSM-IV (Hogrefe).
32. Biswal, B., Yetkin, F.Z., Haughton, V.M., and Hyde, J.S. (1995). Functional connectivity in the motor cortex of resting human brain using echo-planar MRI. Magn. Reson. Med. *34*, 537–541.
33. Behzadi, Y., Restom, K., Liau, J., and Liu, T.T. (2007). A component based noise correction method (CompCor) for BOLD and perfusion based fMRI. Neuroimage *37*, 90–101.
34. Qing, Z., Dong, Z., Li, S., Zang, Y., and Liu, D. (2015). Global signal regression has complex effects on regional homogeneity of resting state fMRI signal. Magn. Reson. Imaging *33*, 1306–1313.
35. Yeh, C.J., Tseng, Y.S., Lin, Y.R., Tsai, S.Y., and Huang, T.Y. (2015). Resting-state functional magnetic resonance imaging: the impact of regression analysis. J. Neuroimaging *25*, 117–123.
36. Wong, C.W., Olafsson, V., Tal, O., and Liu, T.T. (2012). Anti-correlated networks, global signal regression, and the effects of caffeine in resting-state functional MRI. Neuroimage *63*, 356–364.
37. Martuzzi, R., Ramani, R., Qiu, M., Shen, X., Papademetris, X., and Constable, R.T. (2011). A whole-brain voxel based measure of intrinsic connectivity contrast reveals local changes in tissue connectivity with anesthetic without a priori assumptions on thresholds or regions of interest. Neuroimage *58*, 1044–1050.
38. Peelle, J.E., Cusack, R., and Henson, R.N.A. (2012). Adjusting for global effects in voxel-based morphometry: gray matter decline in normal aging. Neuroimage *60*, 1503–1516.
39. Forman, S.D., Cohen, J.D., Fitzgerald, M., Eddy, W.F., Mintun, M.A., and Noll, D.C. (1995). Improved assessment of significant activation in functional magnetic resonance imaging (fMRI): use of a cluster-size threshold. Magn. Reson. Med. *33*, 636–647.
40. Lieberman, M.D., and Cunningham, W.A. (2009). Type I and type II error concerns in fMRI research: re-balancing the scale. Soc. Cogn. Affect. Neurosci. *4*, 423–428.

STAR★METHODS

KEY RESOURCES TABLE

REAGENT or RESOURCE	SOURCE	IDENTIFIER
Biological Samples		
16 Human Males with Body Integrity Dysphoria	This paper	N/A
16 Human Males without Body Integrity Dysphoria	This paper	N/A
Deposited Data		
Raw and analyzed data	This paper	N/A
Software and Algorithms		
MATLAB	https://www.mathworks.com	MATLAB
CONN connectivity Toolbox version 18b	[29]	CONN
Unified segmentation algorithm	[30]	N/A
Artifact Detection Tools	http://www.nitrc.org/projects/artifact_detect	ART
Statistical Parametric Mapping version 12	https://www.fil.ion.ucl.ac.uk/spm/	SPM

RESOURCE AVAILABILITY

Lead Contact

Further information and requests for resources should be directed to and will be fulfilled by the Lead Contact, Peter Brugger (peter.brugger@kliniken-valens.ch).

Materials Availability

There are restrictions to the availability of the raw scans of the participants of the current study due to the guidelines of the ethical committee, as participants might be identifiable.

Data and Code Availability

The preprocessed data supporting the current study have not been deposited in a public repository because of the lack of authorization from the ethical committee. Still, they are available from the corresponding authors on request.

Subjects Details

Sixteen men who all desired an amputation of the left leg were recruited from an advertisement posted on the following website http://www.biid-dach.org/. Eight BID individuals were scanned at the Department of Neuroradiology of the University Hospital of Zurich [13]. The other eight BID were scanned at the Neuroradiology Department of the "ASST Grande Ospedale Metropolitano Niguarda" of Milan. Their ages ranged from 28-67 years with a mean of 44.38 years and a standard deviation (SD) of 12.32 years. Their years of education ranged from 13-18 years (mean = 16.06 years, SD = 2.28 years). Table 2 offers an overview of participants' demographic variables and the characteristics of their amputation desire according to an established scale, the Zurich Xenomelia Scale [14] (see below).

The control group consisted of sixteen healthy men. They were pairwise matched to the BID individuals by sex, age (range = 31-62 years, mean = 44.81 years, SD = 8.82 years, paired t-test: $t(15) = -0.11$, $p = 0.915$), years of education (range = 8-18 years, mean = 15 years, SD = 3.38 years, paired t-test: $t(15) = 1.10$, $p = 0.28$). All participants provided written informed consent to take part in the study. The study was approved by the Ethics Committee of the University Hospital of Zurich, and by the Ethical Committee Milano Area C. The study was run in compliance with the guidance provided in the Declaration of Helsinki (1964).

METHOD DETAILS

Clinical assessments and questionnaires

All participants were screened for physical and mental health in standard neurological and neuropsychological examinations and a psychiatric assessment, which included a series of validated instruments and, for the participants with BID, a 2-h structured clinical

interview [31]. The protocol was the same as described in our previous study [13]. A brief follow-up, approximately 1 year after study completion, revealed that two participants had proceeded to amputation in the meantime. Neurological, neuropsychological, and psychiatric examinations proved normal in all participants, including those with BID.

Table 2 lists the scores on the Zurich Xenomelia Scale and its three subscales [14]. The subscore "amputation desire" is the mean score of 4 items enquiring the identity restoration as the primary motivation for the desire for amputation. The subscore "erotic attraction" is the mean score of 4 items asking for the erotic attraction toward amputated bodies. The subscore "pretending behavior" is the mean score of 4 items asking for the inclination to mimic an amputee (e.g., by using wheelchairs or crutches). The "total scale score" is the mean of all the 12 items and quantifies the strength of the desire for amputation. Each item has a Likert-type format, and answers can range from 1 to 6. Two of the 4 items of each subscale are formulated, such that 1 represents the least strong expression of the critical thought or behavior and 6 the strongest expression. For the other 2 items, this assignment is reversed.

Magnetic resonance imaging data acquisition in Zurich

A 3.0 Tesla Philips Achieva whole-body scanner (Philips Medical Systems, Best, the Netherlands) was used to scan participants in Zurich. This scanner was equipped with a transmit-receive body coil and a commercial eight-element sensitivity encoding (SENSE) head coil array. For each participant, two high-resolution T1-weighted scans were acquired, applying a volumetric three-dimensional T1-weighted fast field echo sequence with a spatial resolution of 0.94 × 0.94 × 1.0 mm3 (acquisition matrix: 256 × 256 pixels, 160 slices) and lasted 468 s. Further imaging parameters were field of view, FOV = 240 × 240 mm2; echo time, TE = 3.7 ms; repetition time, TR = 8.06 ms; flip angle = 8°, and sensitivity encoding (SENSE) factor = 2.1. The two scans were co-registered and averaged, thus increasing the signal-to-noise ratio.

For each participant, we also collected resting-state functional MRI (rs-fMRI) spin-echo echo-planar imaging (EPI) scans. Participants were instructed to close their eyes and to let their minds wander. The rs-fMRI scans were obtained in the transversal plane with a spatial resolution of 2.5 × 2.5 × 4.0 mm3 (reconstructed 1.72 × 1.72 × 4.0 mm3). Imaging parameters were: TR = 4 s; TE = 35 ms; FOV = 220 × 220 mm2; slice thickness = 4 mm; number of slices = 40; SENSE factor = 1.8. The duration of the rs-fMRI sequence was 10 min, and 150 brain volumes were obtained for each participant.

Magnetic resonance imaging data acquisition in Milan

For the sample acquired in Milan, we used a 1.5 T General Electric (GE) Signa HD-XT scanner. This scanner was equipped with an Echo Planar Imaging (EPI) gradient-echo sequence (flip angle = 90°; TE = 60 ms, repetition time (TR) = 3,000 ms, field of view (FOV) = 240 × 240 mm2 and matrix size = 64 × 64 pixels). For each participant, we collected a high-resolution T1-weighted image using a 3D-SPGR sequence (flip angle = 20°, TE = 2.92 ms, TR = 9.16 ms, acquisition matrix: 256 X 256 pixels; slice thickness = 1mm, interslice gap = 0mm, and voxel size = 1 × 1 x 1 mm^3). The volumetric MRI scans consisted of 150 slices acquired on oblique sections parallel to the AC-PC line covering the entire brain volume. Rs-fMRI scans were acquired using the following parameters: Flip angle 90°, TE = 60 msec, TR = 3,000 msec, FOV = 280 × 210 mm2; matrix = 96 × 64 pixels). Each volume was composed of 35 contiguous oblique slices acquired along the AC-PC plane (thickness = 4 mm, gap = 0 mm). The duration of the rs-fMRI sequence was 10 min, and 200 brain volumes were obtained for each participant. The instruction given to participants scanned in Milan was the same as that used in Zurich.

QUANTIFICATION AND STATISTICAL ANALYSIS

Rs-fMRI Data preprocessing

Data preprocessing was performed, implementing the default preprocessing pipeline offered by the CONN connectivity Toolbox [29] version 18b implemented in MATLAB (version 2016b, MathWorks, Natick, MA, USA). Rs-fMRI scans were preliminarily slice-time corrected. The realignment of all the rs-fMRI scans to the first one of the series was then performed. T1-weighed images underwent the unified segmentation algorithm [30]. With this procedure, an estimation of the linear and nonlinear normalization of the T1-weighted MRI image was obtained. Estimated transformations were then applied to the functional images. Rs-fMRI scans were then spatially normalized to the Montreal Neurological Institute (MNI) template (voxel resampling to 2 × 2 x 2 mm^3). Consistent with the parameters used in our previous studies [13, 19] smoothing was performed using a Gaussian kernel of 6 mm full width at half maximum. Outliers scans in global signal and movement were identified with the Artifact Detection Tools (ART http://www.nitrc.org/projects/artifact_detect) and were defined as i) those whose scan-to-scan global signal differences was > 2 SD from the mean and ii) those whose compounded measure of movement parameters was > 2 mm scan-to-scan movement. After taking these steps, rs-fMRI scans were band-pass filtered within the range of 0.008 Hz to 0.09 Hz (i.e., the frequency range of physiological importance for measuring spontaneous neuronal activity [32]). The variance related to translations and rotations using the six motion parameters (considered as first-level covariates) was regressed out, thus improving the signal-to-noise ratio. With the use of the CompCor strategy [33], the BOLD signal from the individual white matter and cerebrospinal fluid were also taken as confounds. No mean global signal regression was performed as the interpretation of the negative correlations observed after performing the mean global signal is still a matter of debate [34–36]

Intrinsic functional connectivity of the cortical hubs

At the single-subject level, to map the intrinsic functional connectivity of the cortical hubs, we computed the intrinsic connectivity of individual voxel (ICC) applying the method described in Martuzzi et al. [37] and implemented in the CONN toolbox. Based on network theory

measures, ICC is a correlation-based connectivity approach that is sensitive to detect the presence and quantify the strength of the functional connections of a given voxel to the rest of the gray matter voxels in the brain. As such, ICC is a whole-brain measure that does not require *a priori* definition of any region of interest (ROIs). Another reason for preferring this index over other network degree-centrality indices (e.g., the degree-centrality index [10, 11]) is that ICC does not require to set an arbitrary threshold after correlating the temporal fluctuations of BOLD signals extracted from every brain voxel. ICC represents, therefore, a powerful and wholly automatized data-driven approach.

Individual ICC maps were z-transformed with the Fisher's r-to-z transform function to obtain normally distributed data that allowed group analyses.

To define the altered intrinsic functional connectivity in BID compared with the control groups, the z-transformed ICC maps of two groups were entered into a second-level random-effects analysis. Our design matrix consisted of 3 columns: i) BID individuals z-transformed ICC maps, ii) Controls z-transformed ICC maps, iii) the covariate "Scanner." This covariate was introduced to account for the different scanners with which data have been collected. Note that the number of BID and control individuals tested in Zurich (8 versus 8) and those tested in Milan (8 versus 8) was the same.

Decreased ICC in BID compared with controls, computed with the T-contrast BID < Controls [-1 1 0], indicated a breakdown of the intrinsic functional connectivity in the cortical hubs in the BID individuals. That is, the resulting cortical hubs were less connected to the rest of the brain in BID individuals compared with the controls. The opposite T-contrast, Controls > BID [1 −1 0], did not yield any significant results. The effects were extracted at $p < 0.001$ uncorrected at voxel-wise level and $p < 0.05$ at the cluster-level. The results are shown in Figure 1 and Table 1 of the manuscript.

The BID Mask

The four regions of the AAL atlas corresponding to the lIFGOrb, the rPCL, the rSPL, and the lITG were included in a brain mask that we called "BID mask." It was created with the Anatomy Toolbox implemented in SPM12 for the subsequent structure analyses, described below, aimed at detecting the cortical regions with an altered concentration of gray matter in BID compared with controls (see the Voxel-Based Morphometry analysis).

This mask also included three regions of the AAL3 atlas whose alteration was predicted from previous studies investigating morphological abnormalities in BID individuals compared with the controls. One was the AAL3 region labeled as "right insula" corresponding to the coordinates of the two clusters of the anterior insular cortex (upper cluster: y = 32 x = 25 z = 9, lower cluster: x = 32 y = 20 z = −4) found altered in BID [13]. The other AAL3 regions were the one labeled as "left precentral gyrus" and "left inferior frontal gyrus, opercular" corresponding to the cluster of the ventral premotor cortex (PMv, y = −50 x = 5 z = 22) and the region labeled as "left superior frontal gyrus" corresponding to the cluster of the dorsal premotor cortex (PMd, x = −20 y = −4 z = 58) [5].

Voxel-based Morphometry analysis

The Voxel-Based Morphometry approach was adopted to identify patterns of altered concentration of gray matter in BID individuals compared with controls. The regions lying in the BID mask were considered in these analyses. Data preprocessing and analyses were performed with MATLAB R2016b (Math Works, Natick, MA, USA), and Statistical Parametric Mapping (SPM12, Wellcome Department of Imaging Neuroscience, London, UK). To comply with a standardized procedure, we ran the classic preprocessing batch "preproc_vbm.m" provided by the SPM12 toolbox under the folder "batches." The preprocessing steps were the following: i) Segmentation of the images to identify white and gray matter; ii) Creation of DARTEL templates and estimation of the deformations that produced the best alignment of all the images, performing iterative registrations of all the images to their average; iii) Warping of the gray matter to the MNI space iii) Application of a Jacobian modulation to preserve an absolute regional amount of gray matter from the distortion introduced by the stereotactic normalization; iv) Normalization of Jacobian scaled gray matter images, using the deformations that were previously estimated v) smoothing using a Kernel Gaussian Filter of 8 × 8 x 8 mm, vi) Averaging of smoothed images; v) Thresholding of the tissue average to get an explicit mask; vi) Normalization of the bias-corrected images to the MNI space; vii) Averaging of the normalized bias-corrected maps; viii) Checking of the average images and the explicit masks in the "Check Reg" provided by SPM 12; ix) Computation of the tissue volumes for each subject. The preprocessed subject-specific maps of gray matter were used to examine the anatomical differences between BID individuals and controls in the predicted key regions. We performed a two-sample t-test for each of the voxels lying within the BID mask. Regional values were corrected using the local correlation (ANCOVA) approach that allowed us to establish the group differences for each voxel that cannot be explained by the linear relationship between the amount of gray matter of that voxel and the total amount of gray matter for each participant. Such an approach, supposed to be more flexible than the global proportional scaling [38], was preferred because participants acquired with different scans belonged to the same group.

Consistent with the ICC maps and seed-based FC analyses, the design matrix comprised 3 columns: i) BID preprocessed gray matter maps, ii) Controls preprocessed gray matter maps, iii) the covariate "Scanner."

Atrophies in BID compared with controls are reflected in the T-contrast BID < Controls [-1 1 0] while hypertrophies are reflected in the T-contrast BID > Controls [1 −1 0].

We used the most conservative thresholding method available in SPM ($p < 0.05$ FWE voxel-wise) coupled with a cluster extent threshold of $k > 25$ to further exclude spurious findings. Indeed, false-positive results do not cluster in space [39, 40].

Update

Current Biology
Volume 31, Issue 16, 23 August 2021, Page 3702

DOI: https://doi.org/10.1016/j.cub.2021.07.037

CellPress

Current Biology

Correction

Neural Correlates of Body Integrity Dysphoria

Gianluca Saetta,* Jürgen Hänggi, Martina Gandola, Laura Zapparoli, Gerardo Salvato, Manuela Berlingeri, Maurizio Sberna, Eraldo Paulesu, Gabriella Bottini, and Peter Brugger*

*Correspondence: gianluca.saetta@gmail.com (G.S.), peter.brugger@kliniken-valens.ch (P.B.)

https://doi.org/10.1016/j.cub.2021.07.037

(Current Biology *30*, 2191–2195.e1–e3; June 8, 2020)

We noticed a typo concerning a finding that we had considered to be too peripheral to be discussed in the original manuscript. In Figure 1, the acronym ''IITG'' (left inferior temporal gyrus) should be ''ISTG'' (left *superior* temporal gyrus). While the MNI coordinates for this region are correctly provided in Table 1 [x = −60, y = −44, z = 16], this region corresponds to the superior temporal gyrus. Also, on page 2 of the manuscript (left column, first line), ''inferior temporal gyrus'' should be referred to as ''*superior* temporal gyrus.'' This error has no effect on the main conclusions of the paper. The authors apologize for any confusion this may have caused.

